Published in final edited form as:
FASEB J. 2007 December ; 21(14): 4077–4086. doi:10.1096/fj.07-8396com.

N-tert-butyl hydroxylamine, a mitochondrial antioxidant, protects human retinal pigment epithelial cells from iron overload: relevance to macular degeneration

Ludmila A. Voloboueva, **David W. Killilea**, **Hani Atamna**, and **Bruce N. Ames**
Children's Hospital Oakland Research Institute, Nutrition and Metabolism Center, Oakland, California, USA

Abstract

Age-related macular degeneration (AMD) is the leading cause of severe visual impairment in the elderly in developed countries. AMD patients have elevated levels of iron within the retinal pigment epithelia (RPE), which may lead to oxidative damage to mitochondria, disruption of retinal metabolism, and vision impairment or loss. As a possible model for iron-induced AMD, we investigated the effects of excess iron in cultured human fetal RPE cells on oxidant levels and mitochondrial cytochrome *c* oxidase (complex IV) function and tested for protection by *N-tert*-butyl hydroxylamine (Nt-BHA), a known mitochondrial antioxidant. RPE exposure to ferric ammonium citrate resulted in a time- and dose-dependent increase in intracellular iron, which increased oxidant production and decreased glutathione (GSH) levels and mitochondrial complex IV activity. NtBHA addition to iron-overloaded RPE cells led to a reduction of intracellular iron content, oxidative stress, and partial restoration of complex IV activity and GSH content. NtBHA might be useful in AMD due to its potential to reduce oxidative stress, mitochondrial damage, and age-related iron accumulation, which may damage normal RPE function and lead to loss of vision.

Keywords

calcitrol; cognition; depression; nutrition; brain development; cytokine theory

Age-related macular degeneration (AMD) is the leading cause of blindness and visual disability in the elderly in developed countries (1). Retinal iron levels increase with age (2). Moreover, it has been shown that the retinal pigment epithelium (RPE) of AMD patients contains significantly higher iron levels than do disease-free retinas (3). Elevated levels of cellular iron are known to cause oxidative damage to mitochondria (4) and cell injury (5–7). Epidemiological studies suggest that environmental factors such as smoking, low dietary antioxidants, and sunlight exposure, all of which are associated with oxidative stress, may contribute to the development of AMD (8–11).

The degeneration of RPE cells is often observed in the early stages of AMD before the degeneration of photoreceptors and vision loss (12,13). RPE is a monolayer of cells forming the blood-retinal barrier that performs many crucial functions such as metabolite transport to photoreceptors and phagocytosis of photoreceptor outer segments (14). RPE is exposed to conditions that promote formation of oxidants, including high oxygen tension (15), direct exposure to sunlight (11,16), and high metabolic activity (17–19). The phagocytosis of

1Correspondence: Children's Hospital Oakland Research Institute, Nutrition and Metabolism Center, 5700 Martin Luther King Jr. Way, Oakland, CA 94609-1673, USA. E-mail: bames@chori.org.

photoreceptor outer segments also imposes a significant oxidative load on RPE cells (17,18). Photoreceptor membranes contain the highest amount of docosahexaenoic acid and other polyunsaturated fatty acids among all body tissues (20). These fatty acids are highly susceptible to oxidative damage and participate in oxidative chain reactions that are facilitated by the higher levels of light and oxygen (21). Moreover, antioxidant defense mechanisms are known to decline with age (10), which may further contribute to an increase in RPE susceptibility to oxidative damage.

The importance of normal iron homeostasis is emphasized by the facts that retinal dysfunction has been observed in some pathological conditions due to the lack of iron (22) and an excess of iron (23–27). Although the subcellular pattern of iron distribution has not been investigated in RPE cells, mitochondria are particularly prone to iron imbalances because of their involvement in heme and iron-sulfur synthesis (4,28,29). Mitochondria are an important cellular target of oxidative stress in RPE (30), and iron excess and iron deficiency can both further enhance the rate of oxidant production and mitochondrial degeneration (4). Pathological alterations in RPE mitochondria of AMD patients have been reported recently and RPE mitochondria have been suggested as a new target for AMD treatment (31). RPE plays a central role in transport of iron from choriocapillaris to photoreceptors (32,33), and dysfunction in retinal iron transport has been shown to promote iron accumulation and retinal degeneration (3,34–36).

The basis for our present study is that *N-tert*-butyl hydroxylamine (NtBHA) is known to delay cellular senescence and protects mitochondria function both *in vitro* and *in vivo* (37,38). NtBHA attenuates senescence-and oxidant-induced iron accumulation in human fibroblasts *in vitro* (39). NtBHA has also been shown to protect against the oxidative damage of ionizing radiation (40) and the oxidation and apoptosis due to heat shock (41). NtBHA is a decomposition product of a free radical scavenger phenyl-*N-tert*-butyl nitrone and has been shown to be more effective in attenuating signs of cellular senescence than the parent compound (37).

MATERIALS AND METHODS

Reagents

Unless stated otherwise, reagents were purchased from Sigma Chemical Company (St. Louis, MO, USA). The production method of NtBHA by Sigma Chemical Company has changed (personal communication with Sigma Technical Service), and we found that this new product was toxic to cells (data not shown); an alternative source of NtBHA (Vitaspace, Central Islip, NY, USA) is well tolerated by cells.

Human fetal RPE cell culture (42)

Research protocols were approved by the University of California Committee for the Protection of Human Subjects and followed the tenets of the Declaration of Helsinki. Fetal eyes were obtained by an independent procurer (Advanced Bioscience Resources, Alameda, CA, USA). Human fetal eyes of nominal gestation of 15–17 wk were dissected within several hours after enucleation, and RPE cell cultures were prepared and grown in RPE culture medium (see below) using Trans-well filters as described (43). After 3–5 wk on Transwell filters, RPE cells acquired a typical cobblestone shape and demonstrated sharp cell boundary and occludin distribution characteristic of the intact confluent RPE cultures (42). RPE cells of second or third passages grown on extracellular matrix-coated Transwell filters for 4–5 wk were used for studies.

Iron overload of cells and treatment with NtBHA

Ferric ammonium citrate (FAC), a soluble ferric iron complex, was used to load RPE with iron. FAC has been used to increase intracellular iron in cultured cells (44) and in brain tissues (45). RPE cells were incubated with different concentrations of FAC for 1–5 days at 37°C, followed by washing with cell culture medium to remove excess iron, then treating the RPE with different concentrations of NtBHA for 16 h.

Assay of oxidants in iron-overloaded RPE

Oxidants in iron-stressed RPE were estimated with the nonfluorescent dye 2′7′-dichlorodihydrofluorescein (H_2DCF) diacetate, (Molecular Probes, Eugene, OR, USA), a nonpolar compound that is converted by cellular esterases to the polar and membrane-impermeable derivative H_2DCF. H_2DCF is oxidized by intracellular oxidants to the highly fluorescent 2′,7′-DCF (46). After treatment, cells were washed once with minimum essential medium (Invitrogen) and incubated with 20 μM H_2DCF diacetate in the dark at 37°C for 30 min. The cells were then washed once with minimum essential medium, and each Transwell filter was scanned (485 nm excitation, 535 nm emission) with a Wallac 1420 multilabel counter (PerkinElmer, Fremont, CA, USA) as described (43). Background fluorescence of cells without H_2DCF diacetate was subtracted. Confluent RPE cells with regular shape and size plated at the same density on the same day were used in each experiment. Each Transwell filter was scanned at 25 areas of rectangularly arranged 5 × 5 pattern with 1 mm intervals and a beam area of ~1 mm^2 (bottom scanning). The averaged fluorescence intensities were expressed relative to control values.

Assay of intracellular pool of labile iron

The labile iron pool was measured using calcein, an iron-sensitive fluorescent probe. Calcein fluorescence is quenched on binding to free intracellular iron ions (47). After treatment with different concentrations of NtBHA and iron (see above), RPE cells were rinsed twice with cell culture medium, then incubated with 250 nM calcein-AM (Molecular Probes) and incubated in minimum essential medium for 15 min at room temperature in the dark. RPE cells were rinsed once, returned to standard culture medium, and equilibrated for 30–40 min before assay of fluorescence. To check for potential changes in dye loading, RPE cells were incubated with 5 μM fluorescein diacetate (Molecular Probes) for 15 min in the dark and rinsed once with minimum essential medium before measurement. The fluorescence measurement protocol for both calcein and fluorescein was similar to that described for DCF measurements above.

Assay of intracellular iron

The iron content of samples was assayed by inductively coupled plasma atomic emission spectrometry as described previously (39). RPE cells were rinsed twice with growth medium and once with ice-cold PBS, scraped into water, and digested in 70% HNO_3 overnight at 60° C with orbital shaking at 250 rpm. Lysates were then diluted with water to 5% HNO_3 and analyzed by inductively coupled plasma atomic emission spectrometry (Varian Vista Pro, Varian, Palo Alto, CA, USA). Elemental values were calibrated using National Institute for Standards and Technology traceable elemental standards (Sigma) and validated using National Institute for Standards and Technology traceable reference material (sample 1577b bovine liver; National Institute for Standards and Technology, Gaithersburg, MD, USA). Lithium (50 parts/million) was used as an ionization buffer and yttrium and scandium (5 parts/million) were used as internal standards. All reagents and plastic ware were routinely tested for trace metals. Data was collected and summarized using native software (ICP Expert, version 3.1). Iron content was normalized to protein levels of RPE cells, which was measured with a bicinchoninic acid-based protein assay kit (Pierce Chemical Company, Rockford, IL, USA).

Western blot assay of the content of ferritin and transferrin receptor

RPE cells (1×10^6) were lysed in 10 mM Tris-ethylenediamine tetraacetic acid (EDTA) and 1% sodium dodecyl sulfate (SDS) with protease inhibitor cocktail (Sigma #P2714). Equal amounts of protein (10–20 μg) were loaded on precast SDS/PAGE gels (Cambrex Bio Science Inc., Rockland, ME, USA). Resolved proteins were transferred from SDS gel to polyvinylidene fluoride membranes (Millipore Corporation, Bedford, MA, USA) using the Trans-Blot Semi-Dry Electrophoretic Transfer Cell (Bio-Rad, Hercules, CA, USA). The membranes were incubated with mouse anti-human transferrin receptor antibody (1:1000 dilution, BD Biosciences, Franklin Lakes, NJ, USA) or sheep anti-human ferritin antibody (1:100 dilution, The Binding Site Ltd., Birmingham, UK) overnight at 4°C. The blots were further labeled with the corresponding horseradish peroxidase-conjugated secondary antibodies (1:500 dilution, Santa Cruz Biotechnology, Inc., Santa Cruz, CA, USA). Membranes were exposed to enhanced chemiluminescent reagent (NEN Life Sciences, Boston, MA, USA) and visualized with film. For normalization of protein loading, the membranes were stripped in Restore Western Stripping reagent (Pierce) and reprobed with mouse anti-human β-actin antibody (1:3000 dilution, Sigma) and goat anti-mouse secondary antibody (1:500 dilution, Santa Cruz Biotechnology, Inc.).

Measuring the effect of iron overload and NtBHA on cell viability

RPE cultures were assayed for cell viability by double labeling with SYTO Green and SYTOX Orange (Molecular Probes) as described (43). Briefly, the RPE cells were incubated with 5 μM SYTOX Orange and 5 μM SYTO Green for 20 min at 37°C. RPE cells were visualized using FITC and TRITC fluorescence filter cubes, respectively, on Axiovert 25 microscope (Carl Zeiss, Jena, Germany) with a charge-coupled device digital camera (Diagnostic Instruments, Sterling Heights, MI, USA) and quantitated with Photoshop 7.0 (Adobe Systems, San Jose, CA, USA).

Assay of glutathione content of RPE

RPE cells (1×106) were acidified in 10% (w/v, 0.25 ml) perchloric acid containing 5 μM EDTA. The cellular concentration of glutathione (GSH), the most important endogenous antioxidant, was assayed according to the methods of Fariss and Reed using an HPLC separation technique as described previously (43,48). GSH content was normalized to the protein content of the RPE cells.

Assay of cytochrome *c* oxidase complex IV

RPE cells from each Transwell were scraped into 180 μl of ice-cold mitochondrial isolation buffer (210 mM mannitol, 70 mM sucrose, 5 mM 4-(2-hydroxyethyl)-1-piperazineethanesulfonic acid (HEPES), 1 mM EDTA, 1/50 dilution of protease inhibitor (Sigma #P-8340), pH adjusted to 7.35 with KOH). RPE cells from three or four duplicate Transwells were combined and homogenized with 12 strokes of a Dounce homogenizer. The resulting lysate was centrifuged in the cold at 1000 *g* for 10 min. The pellet was discarded and the supernatant was centrifuged in the cold at 12,000 *g* for 15 min. The resulting mitochondrial-enriched fraction was washed with isolation buffer (minus EDTA) and repelleted. The protein content of the pellet was measured using bicinchoninic acid protein assay reagent kit (Pierce). Complex IV activity was assayed using a Cytochrome *c* Oxidase Assay Kit (CYTOX-OX1; Sigma) with slight modification for use of a microplate reader. Briefly, the mitochondria-enriched pellet was resuspended in 80 μl of assay buffer, 190 μl of enzyme dilution buffer was dispensed in several wells of 90-well assay plate, and 15 μl of mitochondrial suspension from different treatment conditions was added to each well. The reaction was started simultaneously in several wells by dispensing 20 μl of reduced ferrocytochrome *c* substrate (0.22 mM) solution using a multipipetor. The decrease in the absorption at 550 nm was measured after a 5 s delay

for mixing by shaking at 10 s intervals with six readings. A microplate spectrophotometer, Spectra Max 340 (Molecular Devices, Sunnyvale, CA, USA) with SoftMax Pro was used for data collection and analysis.

Statistical analysis

Statistical significance ($P \leq 0.05$) was determined by the unpaired 2-tailed Student's *t* test using Prism software, version 4.0a (GraphPad Software, San Diego, CA, USA). Plot values represent mean ± SD of the indicated number of measurements.

RESULTS

Iron overload in RPE cells

RPE cells were incubated with 250 μM FAC for 1, 2, 3, and 4 days, resulting in a dose-dependent 16-fold ($P<0.001$, $n=3$), 30-fold ($P<0.001$, $n=3$), 36-fold ($P<0.001$, $n=3$), and 48-fold ($P<0.001$, $n=3$) increase in intracellular iron, respectively, as shown in Fig. 1. Treatment with 250 μM FAC for up to 4 days did not reduce RPE cell viability as indicated by the absence of cell death-specific SYTOX red staining in three separate experiments in duplicate from three different donors (data not shown). The levels of intracellular oxidants significantly increased after treatment of RPE cells with FAC at concentrations of 250 μM, 500 μM, and 1 mM for 4 days by 1.8-fold ($P<0.001$, $n=6$), 1.9-fold ($P<0.001$, $n=6$), and 1.9-fold ($P<0.001$, $n=6$), respectively (Fig. 2*A*). Over the 5 days of exposure to 250 μM FAC, the level of oxidants in cells, as measured by H_2DCF, increased by 1.4-fold ($P=0.005$, $n=6$, day 1), 1.35-fold ($P<0.001$, $n=6$, day 2), 1.7-fold ($P<0.001$, $n=6$, day 3), and 1.9-fold ($P<0.001$, $n=6$, days 4 and 5), respectively (Fig. 2*B*). Four days at 250 μM FAC treatment was used to investigate the effects of iron overload in subsequent experiments.

Effects of NtBHA on the levels of total and intracellular labile iron and oxidative stress in RPE cells

Posttreatment of iron-loaded RPE cells with 250 μM NtBHA for 16 h promoted a significant 19% reduction ($P=0.006$) in the levels of intracellular total iron compared with posttreatment without NtBHA, as shown in Fig. 3*A*. To examine changes in the small pool of labile iron with the cells, the iron-sensitive fluorescence probe calcein was used (Fig. 3*B*); calcein fluorescence inversely correlates with the levels of labile iron (47). FAC treatment (250 μM) for 4 days resulted in a significant 17% ($P<0.001$, $n=6$) decrease in the levels of calcein fluorescence, indicating an increase in labile iron within the cell. Posttreatment with 250 μM NtBHA of iron-treated RPE cells for 16 h caused an increase of 23% ($P<0.001$, $n=7$) in the level of calcein fluorescence relative to NtBHA-free cell medium, indicating decreased levels of labile iron (Fig. 3*B*). NtBHA post-treatment was found to attenuate the FAC-induced levels of intracellular oxidants in a dose-dependent manner (Fig. 3*C*). No significant changes were seen at 50 or 100 μM NtBHA concentrations, but posttreatments with 250 μM and 500 μM NtBHA for 16 h caused a significant reduction by 45% ($P<0.001$, $n=6$) and 46% ($P=0.002$, $n=6$), respectively, in the level of oxidants in iron-overloaded RPE cells compared with RPE cells without NtBHA treatment (Fig. 3*C*). The 250 μM NtBHA treatment of control RPE cells did not induce significant changes in the levels of intracellular labile iron, and this concentration was used in further cellular assays to investigate protective effects of NtBHA in iron-overloaded RPE cells.

Because both calcein and DCF fluorescence can be affected by dye loading and esterase activity in differently RPE treated cells, we used a control fluorescein diacetate (FDA) dye to check for those potential changes. FDA is structurally similar to calcein-AM and, like H_2DCF diacetate and calcein-AM, is practically nonfluorescent until its diacetate moiety is removed by intracellular esterases, but is not affected by iron or free radicals. As demonstrated in Fig.

3*D*, different treatments promoted no significant changes in fluorescein signal, indicating that the changes observed in DCF and calcein fluorescence were not associated with changes in RPE dye loading.

Cell viability assays were performed using SYTO/SYTOX double labeling, which efficiently demonstrated oxidant-induced RPE cell death in our previous studies and indicated <1% cell death in control untreated RPE cultures (43). The percentage of SYTOX-positive dead RPE cells remained below 1% after 1–5 days of 250 μM FAC treatment and after NtBHA posttreatment of control and iron-overloaded RPE cells, thus demonstrating that changes in cell viability were not contributing to iron and oxidative stress changes induced by these treatments.

Effects of NtBHA on GSH levels in RPE

The effects of iron overload and NtBHA posttreatment on the levels of GSH, one of the major cellular antioxidants, were investigated (Fig. 4). GSH levels were increased by 11% (P=0.03, n=5) after treatment of RPE cells with 250 μM NtBHA for 16 h. Treatment with 250 μM FAC (4 days) decreased intracellular GSH levels by 34% (P<0.001, n=5). Posttreatment of iron-overloaded RPE cells with 250 μM NtBHA for 16 h caused a significant increase in GSH levels by 45% (P<0.001, n=5) relative to RPE cells without NtBHA. The results of both the DCF and GSH assays support the notion that NtBHA posttreatment might protect RPE cells against the iron-induced oxidative damage through antioxidant mechanisms.

FAC and NtBHA-mediated changes in transferrin receptor and ferritin levels

The involvement of two iron-associated proteins, transferrin receptor and ferritin, in the changes observed in total and cellular labile iron and in the effects of iron overload and NtBHA posttreatment was investigated by assaying their levels of expression. Iron overload suppressed expression levels of transferrin receptor, but 250 μM NtBHA promoted no observable changes compared with NtBHA-free treatment, as shown in Fig. 5*A*. Iron treatment also promoted strong expression of the iron storage protein ferritin. Posttreatments with 250 μM NtBHA caused an decrease of 48% (P<0.01, n=3) in ferritin levels compared with control untreated samples, but promoted no significant changes in iron-overloaded RPE cells (Fig. 5*A*, *B*).

Effects of NtBHA on RPE complex IV activity

Iron overload promoted increased levels of oxidants in RPE cells. Since oxidative stress is known to decrease the activity of mitochondrial enzymes (4,49), the effects of iron overload on the levels of mitochondrial complex IV activity were measured (Fig. 6). Complex IV activity in 250 μM FAC-treated RPE cells was significantly reduced by 20%(P=0.01, n=3), as shown in Fig. 6. Posttreatment of iron-treated RPE cells with 250 μM NtBHA resulted in a significant 21% (P=0.008, n=3) increase in the levels of complex IV activity compared with treatment without NtBHA.

DISCUSSION

Iron overload is observed in RPE of AMD patients (3). Excess iron, if not stored in ferritin, can provide a potent catalyst for oxidant formation (50) and mitochondrial damage (4). It is widely accepted that the iron used in the outer mammalian retina is transported from the circulation by the RPE cells (32,51). Iron overload observed in RPE of AMD patients (3) can have potentially damaging effects on RPE function and physiology, which might disrupt iron transport to the outer retina.

RPE cells exposed to elevated (250 μM) levels of iron had increased levels of total intracellular iron (Fig. 1). Iron overload in RPE cells promoted increased rates of cellular oxidant production

in a time- and concentration-dependent manner (Fig. 2) and decreased the levels of GSH, a major intracellular antioxidant (Fig. 4). In our experiments, ROS levels did not significantly change after 3 days of iron exposure (Fig. 2*B*) despite a progressive increase in iron levels (Fig. 1). Such stabilization of the RPE redox state can be due to up-regulation of various redox-sensitive transcription factors such as Nrf2, AP1, and NF-kappa B, which promote transcriptional activation of a score of genes involved in attenuation of oxidative stress. We also observed a significant increase in the size of the labile intracellular iron pool in iron-treated RPE cells after 4 days (Fig. 3), suggesting that a small fraction of the iron taken up by the cells is not stored in ferritin and is free to catalyze oxidative damage.

The iron concentrations used in our experiments, 250 μM, could be relevant to the range of concentrations which RPE cells experience under different pathological conditions. Transferrin-bound iron in blood plasma ranges from 9 to 30 μM (45). Drusen of AMD patients contain amyloid-β aggregates (52). Amyloid-β aggregates in Alzheimer disease brain contain iron concentrations approaching 1 mM in Alzheimer patients (53). It seems plausible that amyloid-β in drusen may also contain high iron. The association between Alzheimer disease and AMD, however, is weak (54). RPE is a phagocytic tissue able to phagocytose or endocytose surrounding material, including amyloid-β, which presumably would also be true for amyloid-β-containing heme (55). However, it should be noted that the model used in these studies was a short-term one, with rapid iron loading but minimal cell death. It is unclear how changes in iron homeostasis in our experiments compare to the decades-long, gradual iron overload that develops in AMD patients.

Excess iron increases mitochondrial oxidant stress (4), and mitochondria are a primary target of oxidative stress in RPE cells (30). Excess iron in RPE cells caused a significant decrease in mitochondrial complex IV activity (Fig. 6). Complex IV activity is decreased in aging (56) upon exposure to aldehydes from lipid peroxidation (57) in wet AMD (58) and in Alzheimer patients compared with disease-free patients (59).

We tested the protective effect on iron-stressed RPE cells of NtBHA, an antioxidant that has been shown in our lab to attenuate in human fibroblasts senescence-induced cellular iron accumulation (39) and mitochondrial damage induced by senescence (37,38). NtBHA has also been shown to delay senescence-associated mitochondrial decay, reduce levels of intracellular oxidants, increase the GSH/GSSG ratio, and decrease senescence-associated iron accumulation in other cell types (37–39). Posttreatment with NtBHA decreased FAC-induced iron overload (Fig. 3), decreased the levels of oxidative stress (Fig. 2), partially reversed the iron-induced increase in the levels of calcein-chelatable intracellular iron (Fig. 3), increased GSH in iron-treated RPE cells (Fig. 4), and partially restored mitochondrial complex IV activity in iron-overloaded RPE cells (Fig. 6). In our experiments, we observed stronger NtBHA-induced reversal of labile iron levels in iron-overloaded RPE cells compared with total iron levels. This is likely due to the fact that the labile iron pool is small and more readily affected by NtBHA-induced changes in iron transport compared with the larger total iron pool that is preferentially concentrated within ferritin molecules.

NtBHA was proposed to protect mitochondrial function by undergoing redox cycling in the mitochondrial electron transport chain (38) and thus appears to be a mitochondrial-targeted antioxidant. Mitochondrial-targeted antioxidants, but not their nonspecific analogs, have been demonstrated to prevent oxidant-induced iron overload (60). The mechanism by which NtBHA decreases the excess level of intracellular iron in fibroblasts or RPE cells is unknown.

Iron metabolism and transport in RPE have not been studied extensively. Most mammalian tissues employ transferrin receptors for the uptake of transferrin-bound iron. RPE expresses both transferrin and transferrin receptors (51). It has been suggested that RPE cells transport

iron from the choroidal blood supply to the subretinal space by a process of transcytosis using RPE-synthesized and excreted transferrin molecules (32,51). The iron export protein ferroportin has been immunolocalized in RPE cells (61). Ferroportin exports ferrous iron, which must be oxidized to its ferric form to be accepted by transferrin molecules (62,63). Ferroportin is thus believed to cooperate with ferroxidases, ceruloplasmin, and hephaestin. The observation that ceruloplasmin and hephaestin deficiency promotes iron accumulation in RPE suggests that ferroportin-associated iron transport is present in RPE cells (36,61,64). Ferritin, an iron storage protein, is expressed in high levels in RPE cells (51). In our experiments, iron treatment strongly induced ferritin and suppressed transferrin receptor expression in RPE cells (Fig. 5), reflecting the respective storage and iron import functions of those proteins. We did not observe significant changes in expression levels of transferrin receptors or ferritin with NtBHA treatment of iron-overloaded cells. However, NtBHA treatment of RPE cells not loaded with iron showed a reduction in levels of ferritin expression (Fig. 5). It has been shown that increased rates of iron efflux promote degradation of ferritin molecules in order to maintain the normal range of intracellular labile iron (65). Thus, the observed NtBHA-induced decrease in ferritin levels in RPE cells not loaded with iron might potentially result from NtBHA-stimulated iron efflux. Because labile iron levels represent only a small fraction of the intracellular iron, this mechanism would not significantly change total iron levels in the short term. In iron-overloaded cells, NtBHA-induced total iron efflux did not promote changes in ferritin levels (Fig. 5), possibly because ferritin complexes remained heavily iron loaded, and thus were not degraded.

The expression of ferritin and transferrin receptors is known to be regulated by iron regulatory proteins (IRP1 and IRP2), which in turn are regulated by labile iron levels. Thus, changes in labile iron would be expected to result in changes in ferritin and transferrin receptor gene expression. However, we did not observe changes in ferritin and transferrin receptor levels in iron-loaded cells after treatment with NtBHA. NtBHA-induced changes in redox cell status, as well as impairment of cellular IRP mechanism by strong iron overload and associated oxidative stress, might be partly responsible for the observed lack of change in gene expression. The canonical concept of IRP regulation of iron metabolism has been significantly overhauled, particularly in the case of iron-transporting cells, by recent studies of new iron regulatory mechanisms (66).

Several mechanisms besides IRP-dependent iron regulation have been identified for regulating expression of genes involved in iron homeostasis based on recent studies. GSH synthesis enzymes are part of the phase-2 regulatory control system to protect against oxidants and can be induced by a variety of agents (67,68). These mechanisms can also explain the observed effects of NtBHA on labile iron regulation in RPE cells. It has been suggested that the export of intracellular complex of GSH and Fe through a GSH transporter multidrug resistance-associated protein (MRP1) can represent a potential mechanism of cellular iron efflux (69). It has also been demonstrated that hsp27, a heat shock protein involved in antioxidant cell protection, reduced iron levels in murine cells *via* a mechanism not involving down-regulation of transferrin receptor expression (70). Because NtBHA is an antioxidant and also increases cellular GSH levels, increased iron efflux may play a significant role in the cytoprotection of iron-loaded RPE cells. So far, only one study demonstrated the presence of an iron exporting system in RPE tissue, namely, the iron transporter ferroportin (61). Regulatory mechanisms of ferroportin transport are not well studied and might potentially involve redox regulation. It is also possible that the well-known transporter DMT-1 may play a role in iron export in RPE, though the presence of DMT-1 in RPE has not been confirmed. Other studies have shown that DMT-1 is regulated by the cellular redox state and so could be affected by NtBHA treatment (71). Further investigation is needed to clarify the complexity of iron metabolism in RPE cells.

The effects of iron overload as a model of AMD in human RPE cells suggest that NtBHA treatment can decrease the levels of total and chelatable iron, iron-induced intracellular oxidative stress, and RPE mitochondrial dysfunction. Understanding the effect and mechanism of this protection might be useful in developing strategies to attenuate AMD in humans.

Acknowledgements

The paper was supported by NIH/BDPE grant R21 EY016101–01 (B.N.A.) and partially supported by Sheldon Miller's NIH grant EY02205 (L.A.V.). We are grateful to Sheldon Miller, Jiankang Liu, Jung Suh, and Ben Huang for advice and to Teresa Klask for editorial assistance.

REFERENCES

1. Harvey PT. Common eye diseases of elderly people: identifying and treating causes of vision loss. Gerontology 2003;49:1–11. [PubMed: 12457044]
2. Hahn P, Ying GS, Beard J, Dunaief JL. Iron levels in human retina: sex difference and increase with age. NeuroReport 2006;17:1803–1806. [PubMed: 17164668]
3. Hahn P, Milam AH, Dunaief JL. Maculas affected by age-related macular degeneration contain increased chelatable iron in the retinal pigment epithelium and Bruch's membrane. Arch. Ophthalmol 2003;121:1099–1105. [PubMed: 12912686]
4. Walter PB, Knutson MD, Paler-Martinez A, Lee S, Xu Y, Viteri FE, Ames BN. Iron deficiency and iron excess damage mitochondria and mitochondrial DNA in rats. Proc. Natl. Acad. Sci. U. S. A 2002;99:2264–2269. [PubMed: 11854522]
5. Meneghini R. Iron homeostasis, oxidative stress, and DNA damage. Free Radic. Biol. Med 1997;23:783–792. [PubMed: 9296456]
6. Henle ES, Luo Y, Gassmann W, Linn S. Oxidative damage to DNA constituents by iron-mediated fenton reactions. The deoxyguanosine family. J. Biol. Chem 1996;271:21177–21186. [PubMed: 8702888]
7. Eaton JW, Qian M. Molecular bases of cellular iron toxicity. Free Radic. Biol. Med 2002;32:833–840. [PubMed: 11978485]
8. Smith W, Assink J, Klein R, Mitchell P, Klaver CC, Klein BE, Hofman A, Jensen S, Wang JJ, de Jong PT. Risk factors for age-related macular degeneration: Pooled findings from three continents. Ophthalmology 2001;108:697–704. [PubMed: 11297486]
9. Seddon JM, Ajani UA, Sperduto RD, Hiller R, Blair N, Burton TC, Farber MD, Gragoudas ES, Haller J, Miller DT, et al. Dietary carotenoids, vitamins A, C, and E, and advanced age-related macular degeneration. Eye Disease Case-control Study Group. JAMA 1994;272:1413–1420. [PubMed: 7933422]
10. Samiec PS, Drews-Botsch C, Flagg EW, Kurtz JC, Sternberg P Jr, Reed RL, Jones DP. Glutathione in human plasma: decline in association with aging, age-related macular degeneration, and diabetes. Free Radic. Biol. Med 1998;24:699–704. [PubMed: 9586798]
11. Cruickshanks KJ, Klein R, Klein BE, Nondahl DM. Sunlight and the 5-year incidence of early age-related maculopathy: the beaver dam eye study. Arch. Ophthalmol 2001;119:246–250. [PubMed: 11176987]
12. Green WR, McDonnell PJ, Yeo JH. Pathologic features of senile macular degeneration. Ophthalmology 1985;92:615–627. [PubMed: 2409504]
13. Hamdi HK, Kenney C. Age-related macular degeneration: a new viewpoint. Front. Biosci 2003;8:e305–e314. [PubMed: 12700041]
14. Marmor, M.; Wolfensberger, T., editors. The Retinal Pigment Epithelium: Function and Disease. New York: Oxford Univ. Press; 1998.
15. Wangsa-Wirawan ND, Linsenmeier RA. Retinal oxygen: fundamental and clinical aspects. Arch. Ophthalmol 2003;121:547–557. [PubMed: 12695252]
16. Beatty S, Koh H, Phil M, Henson D, Boulton M. The role of oxidative stress in the pathogenesis of age-related macular degeneration. Surv. Ophthalmol 2000 0;45:115–134. [PubMed: 11033038]

17. Kennedy CJ, Rakoczy PE, Constable IJ. Lipofuscin of the retinal pigment epithelium: a review. Eye 1995;9:763–771. [PubMed: 8849547]

18. Miceli MV, Liles MR, Newsome DA. Evaluation of oxidative processes in human pigment epithelial cells associated with retinal outer segment phagocytosis. Exp. Cell Res 1994;214:242–249. [PubMed: 8082727]

19. Snodderly DM. Evidence for protection against age-related macular degeneration by carotenoids and antioxidant vitamins. Am. J. Clin. Nutr 1995;62:1448S–1461S. [PubMed: 7495246]

20. Fliesler SJ, Anderson RE. Chemistry and metabolism of lipids in the vertebrate retina. Prog. Lipid. Res 1983;22:79–131. [PubMed: 6348799]

21. Gardner HW. Oxygen radical chemistry of polyunsaturated fatty acids. Free Radic. Biol. Med 1989;7:65–86. [PubMed: 2666279]

22. Lakhanpal V, Schocket SS, Jiji R. Deferoxamine (Desferal)-induced toxic retinal pigmentary degeneration and presumed optic neuropathy. Ophthalmology 1984;91:443–451. [PubMed: 6739047]

23. Doly M, Bonhomme B, Vennat JC. Experimental study of the retinal toxicity of hemoglobinic iron. Ophthalmic Res 1986;18:21–27. [PubMed: 3951802]

24. Rapp, LM.; Wiegand, RD.; Anderson, RE. Ferrous ion-mediated retinal degeneration: role of rod outer segment peroxidation. In: Clayton, RM.; Haywood, J.; Reading, HW.; Wright, A., editors. Problem of Normal and Genetically Abnormal Retinas. New York: Academic; 1982. p. 109-119.

25. Wang ZJ, Lam KW, Lam TT, Tso MO. Iron-induced apoptosis in the photoreceptor cells of rats. Invest. Ophthalmol. Vis. Sci 1998;39:631–633. [PubMed: 9501875]

26. Vergara O, Ogden T, Ryan S. Posterior penetrating injury in the rabbit eye: effect of blood and ferrous ions. Exp. Eye Res 1989;49:1115–1126. [PubMed: 2612587]

27. Tawara A. Transformation and cytotoxicity of iron in siderosis bulbi. Invest. Ophthalmol. Vis. Sci 1986;27:226–236. [PubMed: 3943946]

28. Huang XP, O'Brien PJ, Templeton DM. Mitochondrial involvement in genetically determined transition metal toxicity I. Iron toxicity. Chem. Biol. Interact 2006;163:68–76. [PubMed: 16797509]

29. Atamna H, Walter PB, Ames BN. The role of heme and iron-sulfur clusters in mitochondrial biogenesis, maintenance, and decay with age. Arch. Biochem. Biophys 2002;397:345–353. [PubMed: 11795893]

30. Liang FQ, Godley BF. Oxidative stress-induced mitochondrial DNA damage in human retinal pigment epithelial cells: a possible mechanism for RPE aging and age-related macular degeneration. Exp. Eye Res 2003;76:397–403. [PubMed: 12634104]

31. Feher J, Kovacs I, Artico M, Cavallotti C, Papale A, Balacco Gabrieli C. Mitochondrial alterations of retinal pigment epithelium in age-related macular degeneration. Neurobiol. Aging 2006;27:983–993. [PubMed: 15979212]

32. Hunt RC, Davis AA. Release of iron by human retinal pigment epithelial cells. J. Cell Physiol 1992;152:102–110. [PubMed: 1618912]

33. Yefimova MG, Jeanny JC, Keller N, Sergeant C, Guillonneau X, Beaumont C, Courtois Y. Impaired retinal iron homeostasis associated with defective phagocytosis in Royal College of Surgeons rats. Invest. Ophthalmol. Vis. Sci 2002;43:537–545. [PubMed: 11818402]

34. Miyajima H, Nishimura Y, Mizoguchi K, Sakamoto M, Shimizu T, Honda N. Familial apoceruloplasmin deficiency associated with blepharospasm and retinal degeneration. Neurology 1987;37:761–767. [PubMed: 3574673]

35. Morita H, Ikeda S, Yamamoto K, Morita S, Yoshida K, Nomoto S, Kato M, Yanagisawa N. Hereditary ceruloplasmin deficiency with hemosiderosis: a clinicopathological study of a Japanese family. Ann. Neurol 1995;37:646–656. [PubMed: 7755360]

36. Dunaief JL, Richa C, Franks EP, Schultze RL, Aleman TS, Schenck JF, Zimmerman EA, Brooks DG. Macular degeneration in a patient with aceruloplasminemia, a disease associated with retinal iron overload. Ophthalmology 2005;112:1062–1065. [PubMed: 15882908]

37. Atamna H, Paler-Martinez A, Ames BN. N-t-butyl hydroxylamine, a hydrolysis product of alpha-phenyl-N-t-butyl nitrone, is more potent in delaying senescence in human lung fibroblasts. J. Biol. Chem 2000;275:6741–6748. [PubMed: 10702229]

38. Atamna H, Robinson C, Ingersoll R, Elliott H, Ames BN. N-t-Butyl hydroxylamine is an antioxidant that reverses age-related changes in mitochondria in vivo and in vitro. FASEB J 2001;15:2196–2204. [PubMed: 11641246]
39. Killilea DW, Atamna H, Liao C, Ames BN. Iron accumulation during cellular senescence in human fibroblasts in vitro. Antioxid. Redox Signal 2003;5:507–516. [PubMed: 14580305]
40. Lee JH, Kim IS, Park JW. The use of N-t-butyl hydroxylamine for radioprotection in cultured cells and mice. Carcinogenesis 2004;25:1435–1442. [PubMed: 15016661]
41. Kim HJ, Shin SW, Oh CJ, Lee MH, Yang CH, Park JW. N-t-Butyl hydroxylamine regulates heat shock-induced apoptosis in U937 cells. Redox Rep 2005;10:287–293. [PubMed: 16438800]
42. Maminishkis A, Chen S, Jalickee S, Banzon T, Shi G, Wang FE, Ehalt T, Hammer JA, Miller SS. Confluent monolayers of cultured human fetal retinal pigment epithelium exhibit morphology and physiology of native tissue. Invest. Ophthalmol. Vis. Sci 2006;47:6312–3624.
43. Voloboueva LA, Liu J, Suh JH, Ames BN, Miller SS. (R)-α-lipoic acid protects retinal pigment epithelial cells from oxidative damage. Invest. Ophthalmol. Vis. Sci 2005;46:4302–4310. [PubMed: 16249512]
44. Hoepken HH, Korten T, Robinson SR, Dringen R. Iron accumulation, iron-mediated toxicity and altered levels of ferritin and transferrin receptor in cultured astrocytes during incubation with ferric ammonium citrate. J. Neurochem 2004;88:1194–1202. [PubMed: 15009675]
45. Bishop GM, Robinson SR. Quantitative analysis of cell death and ferritin expression in response to cortical iron: implications for hypoxia-ischemia and stroke. Brain Res 2001;907:175–187. [PubMed: 11430901]
46. Brubacher JL, Bols NC. Chemically de-acetylated 2′,7′-dichlorodihydrofluorescein diacetate as a probe of respiratory burst activity in mononuclear phagocytes. J. Immunol. Methods 2001;251:81–91. [PubMed: 11292484]
47. Epsztejn S, Kakhlon O, Glickstein H, Breuer W, Cabantchik I. Fluorescence analysis of the labile iron pool of mammalian cells. Anal. Biochem 1997;248:31–40. [PubMed: 9177722]
48. Fariss MW, Reed DJ. High-performance liquid chromatography of thiols and disulfides: dinitrophenol derivatives. Methods Enzymol 1987;143:101–109. [PubMed: 3657520]
49. Davis, KJA. Oxidative Damage and Repair: Chemical, Biological and Medical Aspects. Oxford/New York: Pergamon Press; 1991.
50. Gutteridge JM, Halliwell B. Iron toxicity and oxygen radicals. Baillieres Clin. Haematol 1989;2:195–256. [PubMed: 2660928]
51. Yefimova MG, Jeanny JC, Guillonneau X, Keller N, Nguyen-Legros J, Sergeant C, Guillou F, Courtois Y. Iron, ferritin, transferrin, and transferrin receptor in the adult rat retina. Invest. Ophthalmol. Vis. Sci 2000;41:2343–2351. [PubMed: 10892882]
52. Anderson DH, Talaga KC, Rivest AJ, Barron E, Hageman GS, Johnson LV. Characterization of beta amyloid assemblies in drusen: the deposits associated with aging and age-related macular degeneration. Exp. Eye Res 2004;78:243–256. [PubMed: 14729357]
53. Lovell MA, Robertson JD, Teesdale WJ, Campbell JL, Markesbery WR. Copper, iron and zinc in Alzheimer's disease senile plaques. J. Neurol. Sci 1998;158:47–52. [PubMed: 9667777]
54. Roca-Santiago HM, Lago-Bouza JR, Millan-Calenti JC, Gomez-Ulla-Irazazabal F. Alzheimer's disease and age-related macular degeneration. Arch. Soc. Esp. Oftalmol 2006;81:73–78. [PubMed: 16511713]
55. Atamna H, Boyle K. Amyloid-beta peptide binds with heme to form a peroxidase: relationship to the cytopathologies of Alzheimer's disease. Proc. Natl. Acad. Sci. U. S. A 2006;103:3381–3386. [PubMed: 16492752]
56. Paradies G, Ruggiero FM, Petrosillo G, Gadaleta MN, Quagliariello E. Effect of aging and acetyl-L-carnitine on the activity of cytochrome oxidase and adenine nucleotide translocase in rat heart mitochondria. FEBS Lett 1994;350:213–215. [PubMed: 8070566]
57. Chen J, Schenker S, Frosto TA, Henderson GI. Inhibition of cytochrome c oxidase activity by 4-hydroxynonenal (HNE). Role of HNE adduct formation with the enzyme subunits. Biochim. Biophys. Acta 1998;1380:336–344. [PubMed: 9555085]

58. Yu J, Wu L, Xu L. Detection and analysis of mitochondrial DNA mutation and oxidative phosphorylation in age-related macular degeneration patients. J. Fourth Military Med. Univ 2003;24:805–808.
59. Maurer I, Zierz S, Moller HJ. A selective defect of cytochrome c oxidase is present in brain of Alzheimer disease patients. Neurobiol. Aging 2000;21:455–462. [PubMed: 10858595]
60. Dhanasekaran A, Kotamraju S, Kalivendi SV, Matsunaga T, Shang T, Keszler A, Joseph J, Kalyanaraman B. Supplementation of endothelial cells with mitochondria-targeted antioxidants inhibit peroxide-induced mitochondrial iron uptake, oxidative damage, and apoptosis. J. Biol. Chem 2004;279:37575–37587. [PubMed: 15220329]
61. Hahn P, Dentchev T, Qian Y, Rouault T, Harris ZL, Dunaief JL. Immunolocalization and regulation of iron handling proteins ferritin and ferroportin in the retina. Mol. Vis 2004;10:598–607. [PubMed: 15354085]
62. Donovan A, Brownlie A, Zhou Y, Shepard J, Pratt SJ, Moynihan J, Paw BH, Drejer A, Barut B, Zapata A, et al. Positional cloning of zebrafish ferroportin1 identifies a conserved vertebrate iron exporter. Nature 2000;403:776–781. [PubMed: 10693807]
63. McKie AT, Marciani P, Rolfs A, Brennan K, Wehr K, Barrow D, Miret S, Bomford A, Peters TJ, Farzaneh F, et al. A novel duodenal iron-regulated transporter, IREG1, implicated in the basolateral transfer of iron to the circulation. Mol. Cell 2000;5:299–309. [PubMed: 10882071]
64. Hahn P, Qian Y, Dentchev T, Chen L, Beard J, Harris ZL, Dunaief JL. Disruption of ceruloplasmin and hephaestin in mice causes retinal iron overload and retinal degeneration with features of age-related macular degeneration. Proc. Natl. Acad. Sci. U. S. A 2004;101:13850–13855. [PubMed: 15365174]
65. De Domenico I, Vaughn MB, Li L, Bagley D, Musci G, Ward DM, Kaplan J. Ferroportin-mediated mobilization of ferritin iron precedes ferritin degradation by the proteasome. EMBO J 2006;25:5396–5404. [PubMed: 17082767]
66. Dunn LL, Rahmanto YS, Richardson DR. Iron uptake and metabolism in the new millennium. Trends. Cell Biol 2007;17:93–100. [PubMed: 17194590]
67. Kwak MK, Wakabayashi N, Itoh K, Motohashi H, Yamamoto M, Kensler TW. Modulation of gene expression by cancer chemopreventive dithiolethiones through the Keap1-Nrf2 pathway. Identification of novel gene clusters for cell survival. J. Biol. Chem 2003;278:8135–8145. [PubMed: 12506115]
68. Suh JH, Shenvi SV, Dixon BM, Liu H, Jaiswal AK, Liu RM, Hagen TM. Decline in transcriptional activity of Nrf2 causes age-related loss of glutathione synthesis, which is reversible with lipoic acid. Proc. Natl. Acad. Sci. U. S. A 2004;101:3381–3386. [PubMed: 14985508]
69. Watts RN, Hawkins C, Ponka P, Richardson DR. Nitrogen monoxide (NO)-mediated iron release from cells is linked to NO-induced glutathione efflux via multidrug resistance-associated protein 1. Proc. Natl. Acad. Sci. U. S. A 2006;103:7670–7675. [PubMed: 16679408]
70. Chen H, Zheng C, Zhang Y, Chang YZ, Qian ZM, Shen X. Heat shock protein 27 downregulates the transferrin receptor 1-mediated iron uptake. Int. J. Biochem. Cell Biol 2006;38:1402–1416. [PubMed: 16546437]
71. Wetli HA, Buckett PD, Wessling-Resnick M. Small-molecule screening identifies the selanazal drug ebselen as a potent inhibitor of DMT1-mediated iron uptake. Chem. Biol 2006;13:965–972. [PubMed: 16984886]

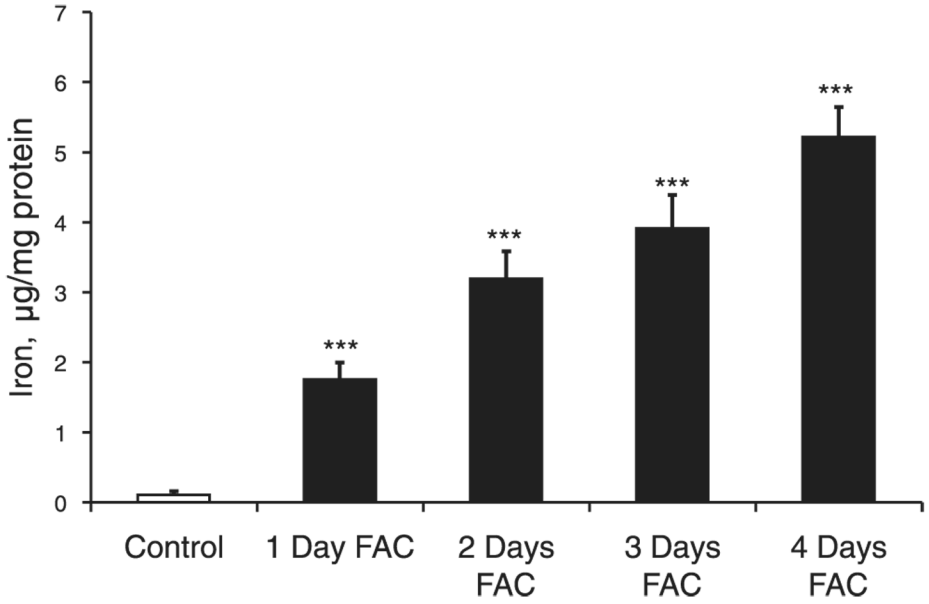

Figure 1.

Time-dependent increase in the levels of total iron in RPE cells treated with 250 µM FAC. Changes in total iron levels were measured using ICP. FAC exposure for 1–4 days promoted a time-dependent increase in the levels of total iron in RPE cells. The data represent mean ± SD of 3 independent experiments (***P<0.001).

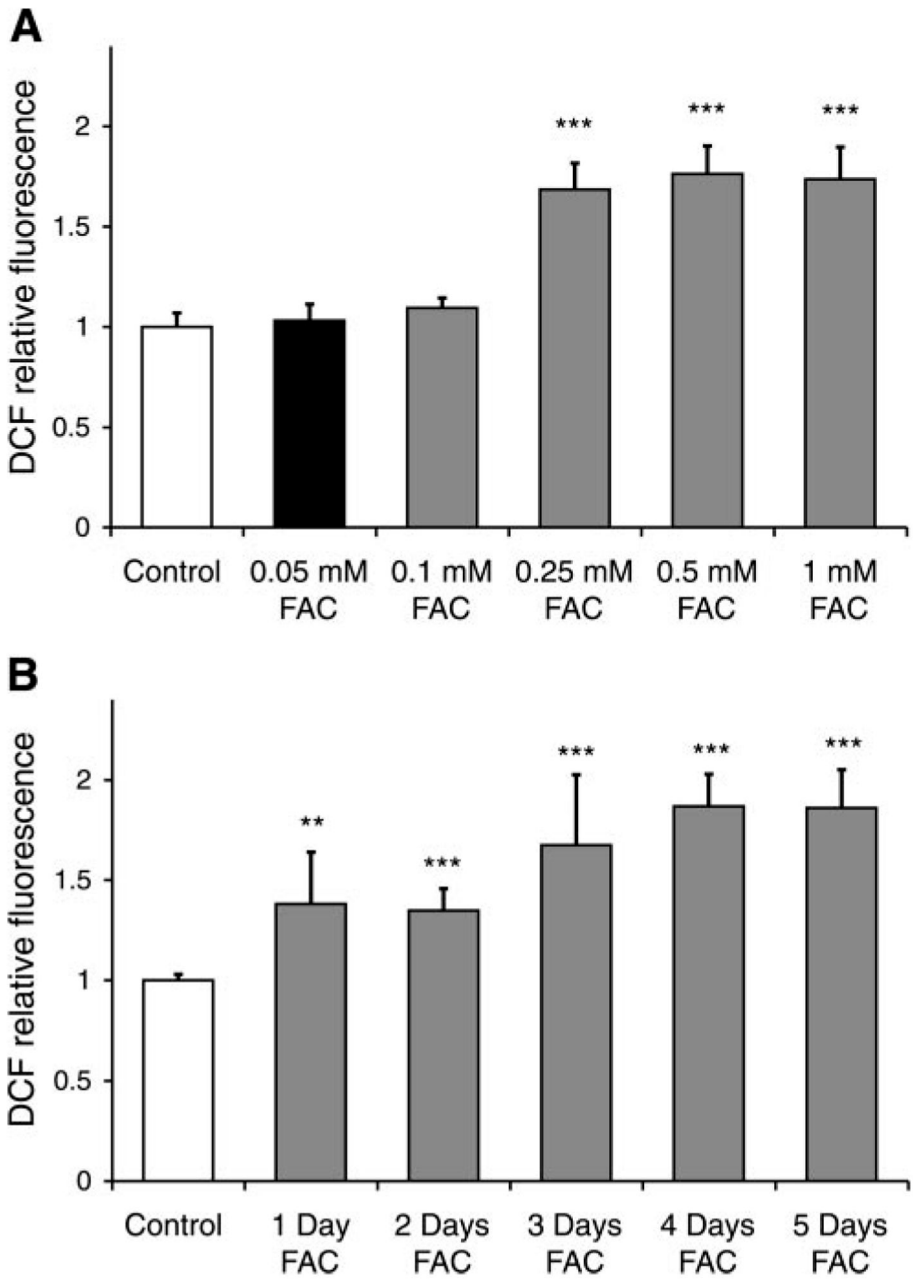

Figure 2.

Iron overload induced dose- and time-dependent increase in the levels of oxidative stress in RPE. *A)* Effect of different concentrations of FAC (4 days' treatment) on the levels of intracellular oxidants. Changes in oxidative stress were measured with the oxidant-sensitive dye H_2DCF. The significant increase in oxidant levels was induced by the concentrations of FAC of 250 μM or greater. The data represent mean ± SD of 6 samples from 3 different experiments (***P<0.001 *vs*. control). *B)* Time-dependent increase in the levels of intracellular oxidants in RPE cells treated with 250 μM FAC. The data represent mean ± SD of 6 samples from 3 different experiments (**P<0.01, ***P<0.001 *vs.* control).

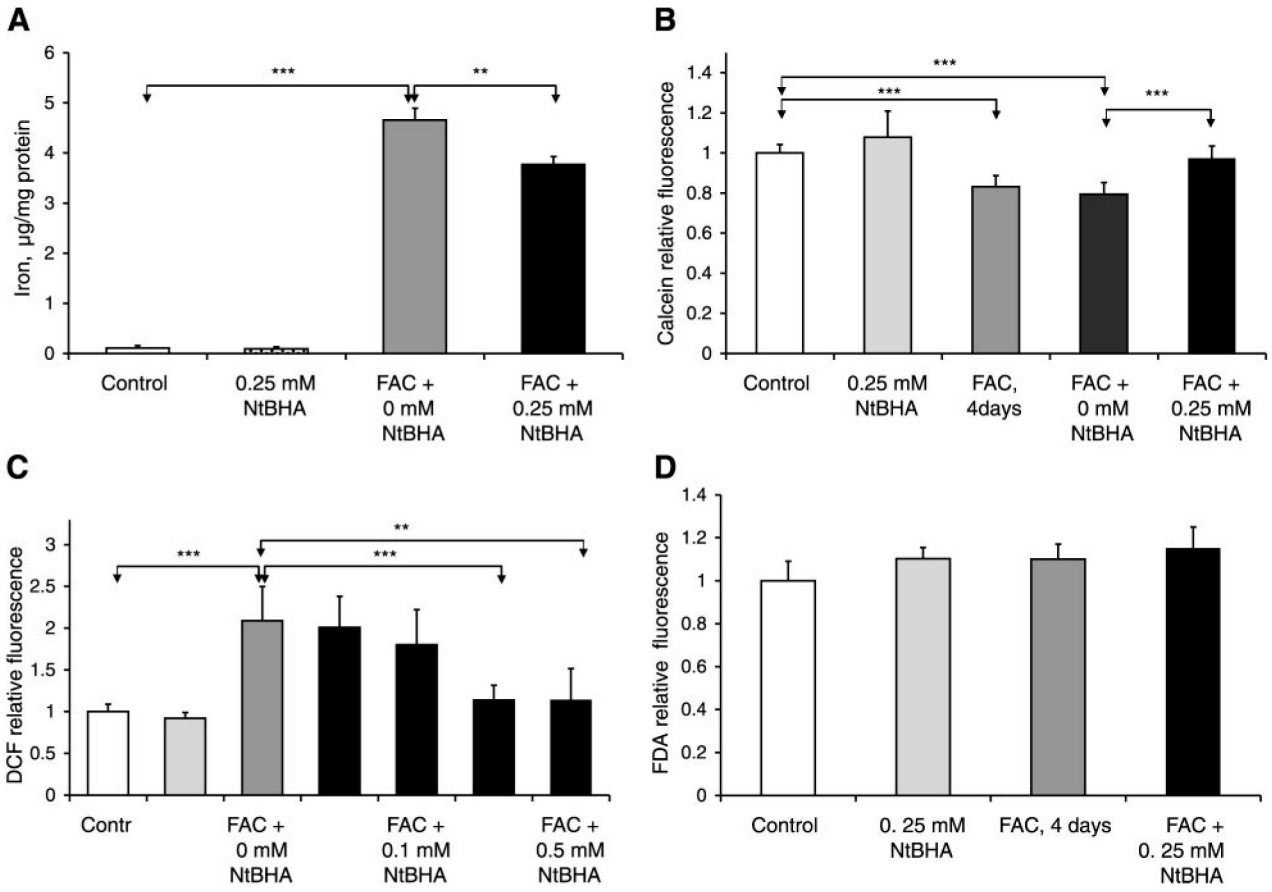

Figure 3.

Effects of NtBHA posttreatment on iron homeostasis and oxidative stress levels in RPE cells. *A)* NtBHA posttreatment resulted in a decrease in levels of total iron in RPE cells treated with FAC (250 µM, 4 days) as determined by ICP. RPE cells were treated with NtBHA (250 µM, 16 h) after FAC exposure, and demonstrated a significant decrease in the levels of total iron compared with RPE cells treated with medium alone (0 µM NtBHA). The data represent mean ± SD of 3 independent experiments (***P*<0.01, ****P*<0.001). *B)* Effect of iron overload and NtBHA posttreatment on the levels of labile iron in RPE cells. Different treatments are indicated as follows: control = untreated RPE cells; NtBHA = RPE cells treated with 250 µM NtBHA; FAC, 4 days = RPE cells treated with 250 µM FAC for 4 days; FAC + 0 µM NtBHA = RPE cells treated with 250 µM FAC for 4 days and posttreated with NtBHA-free cell medium; FAC + 250 µM NtBHA = RPE cells treated with 250 µM FAC for 4 days and posttreated with 250 µM NtBHA. Changes in labile iron levels were measured with Fe-sensitive calcein dye. FAC treatment for 4 days promoted significant decrease in calcein fluorescence, indicating increased labile iron concentration. Treatment with 250 µM NtBHA of iron-loaded cells reduced the levels of intracellular labile iron compared with RPE cells treated with medium alone (0 µM NtBHA). The data represent mean ± SD of 7 samples from 4 independent experiments (****P*<0.001). *C)* Effect of NtBHA posttreatment on the levels of intracellular oxidants in iron-treated RPE cells. RPE cells were treated overnight (16 h) with different concentrations of NtBHA after 4 days of FAC exposure. Changes in oxidant levels were measured with oxidant-sensitive dye H_2DCF. Data are expressed as mean ± SD of 3 independent experiments. Each experiment was performed in duplicate (***P*<0.01, ****P*<0.001). *D)* Fluorescein diacetate dye was used as a control to check for potential changes in RPE dye

loading. Different treatments promoted no significant changes in fluorescein signal indicating no difference in loading differently treated RPE cells with dyes.

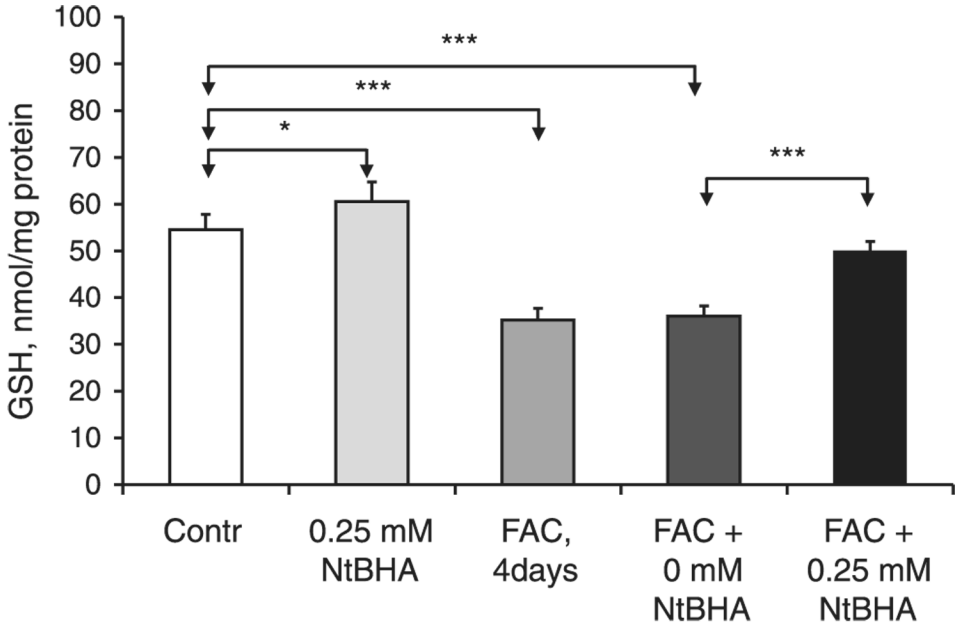

Figure 4.

Effect of iron overload and NtBHA treatment on GSH levels in RPE cells. Control = untreated RPE cells; NtBHA = RPE cells treated with 250 μM NtBHA for 16 h; FAC, 4 days = RPE cells treated with 250 μM FAC for 4 days; FAC + 0 μM NtBHA = RPE cells treated with 250 μM FAC for 4 days and posttreated with NtBHA-free cell medium for 16 h; FAC + 250 μM NtBHA = RPE cells treated with 250 μM FAC for 4 days and posttreated with 250 μM NtBHA for 16 h. NtBHA treatment caused a significant increase in GSH levels in both control and FAC-treated RPE cells. The data represent mean ± SD of 5 samples from 3 different experiments (*P<0.05, ***P<0.001).

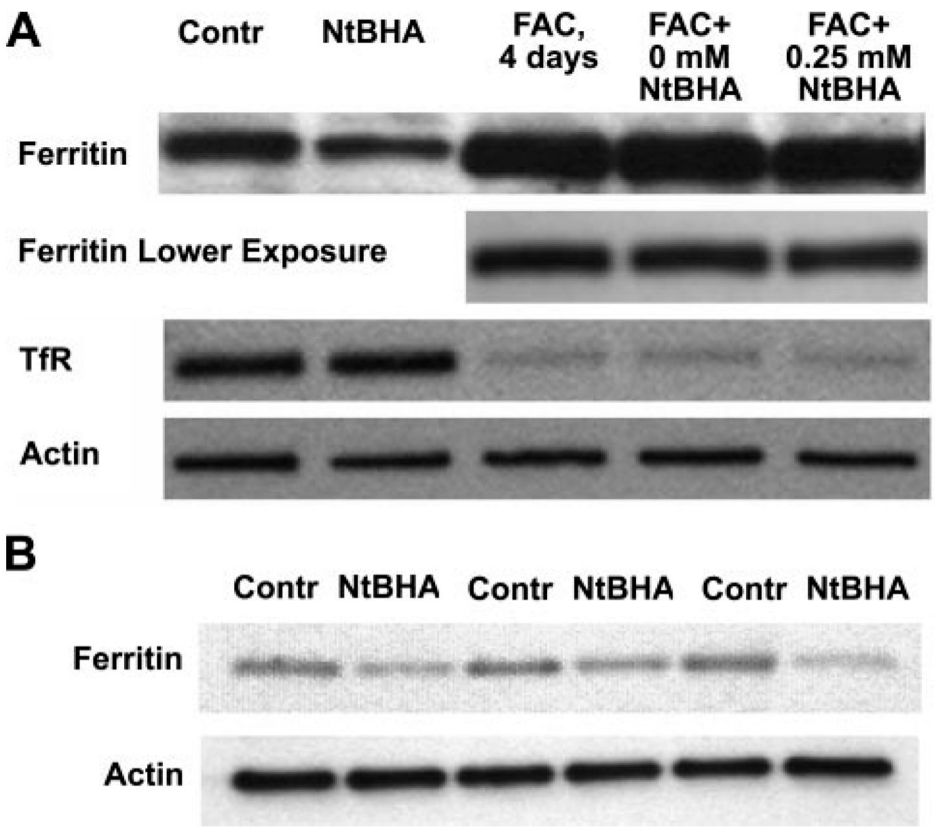

Figure 5.

Effect of iron overload and NtBHA treatment on ferritin and transferrin receptor (TfR) expression in RPE cells. *A)* Different treatments are indicated: Contr = control untreated RPE cells; NtBHA = RPE cells treated with 250 μM NtBHA for 16 h; FAC, 4 days = RPE cells treated with 250 μM FAC for 4 days; FAC + 0 μM NtBHA = RPE cells treated with 250 μM FAC for 4 days, then treated with NtBHA-free cell medium for 16 h; FAC = 250 μM NtBHA = RPE cells treated with 250 μM FAC for 4 days, then treated with 250 μM NtBHA for 16 h. *B)* Effect of NtBHA (250 μM, 16 h) treatment on ferritin levels in RPE cells from 3 different donors.

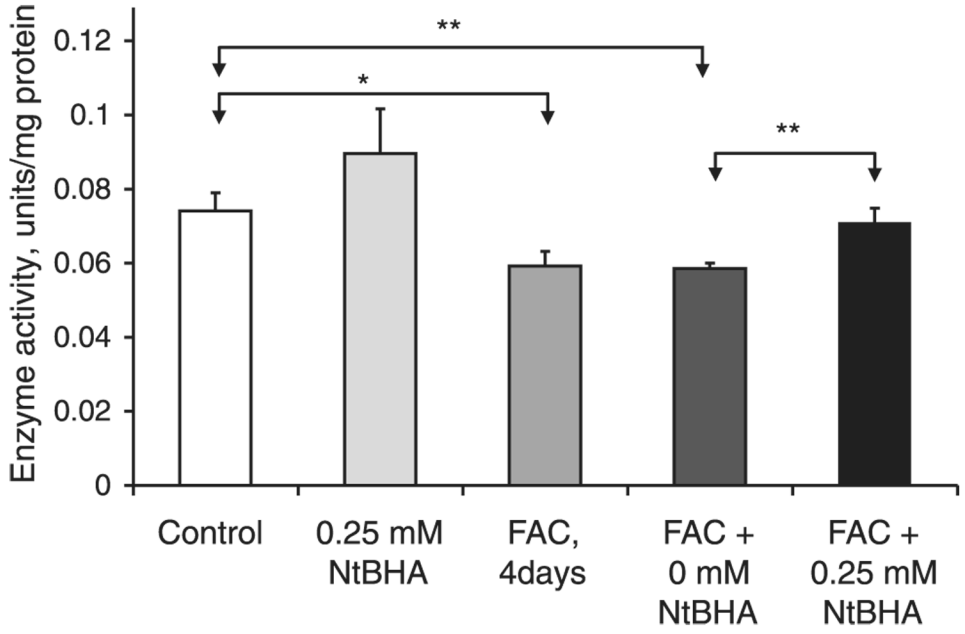

Figure 6.

Effect of iron overload and NtBHA treatment on mitochondrial complex IV activity. Control = untreated RPE cells; NtBHA = RPE cells treated with 250 μM NtBHA; FAC, 4 days = RPE cells treated with 250 μM FAC for 4 days; FAC + 0 μM NtBHA = RPE cells treated with 250 μM FAC for 4 days, then treated with NtBHA-free cell medium; FAC + 250 μM NtBHA = RPE cells treated with 250 μM FAC for 4 days, then treated with 250 μM NtBHA. Changes in the enzyme activity were measured using kinetic colorimetric assay. FAC treatment for 4 days caused a significant decrease in complex IV activity. Treatment with 250 μM NtBHA of iron overloaded cells resulted in a significant increase of complex IV activity compared with RPE cells treated with medium alone (0 μM NtBHA). Iron-loaded RPE cells treated with 250 μM NtBHA demonstrated significantly higher levels of complex IV activity compared with RPE cells treated with medium alone (0 μM NtBHA). The data represent mean ± SD of 3 independent experiments (*P<0.05 *vs*. control, **P<0.01).